

Self-organized criticality in a network of interacting neurons

This content has been downloaded from IOPscience. Please scroll down to see the full text.

J. Stat. Mech. (2013) P04030

(<http://iopscience.iop.org/1742-5468/2013/04/P04030>)

View [the table of contents for this issue](#), or go to the [journal homepage](#) for more

Download details:

IP Address: 130.89.13.208

This content was downloaded on 19/11/2014 at 08:46

Please note that [terms and conditions apply](#).

Self-organized criticality in a network of interacting neurons

J D Cowan¹, J Neuman², B Kiewiet³ and W van Drongelen³

¹ Department of Mathematics, University of Chicago, 5734 South University Avenue, Chicago, IL 60637, USA

² Department of Physics, University of Chicago, 5720 South Ellis Avenue, Chicago, IL 60637, USA

³ Department of Pediatrics, University of Chicago, KCBD 900 East 57th Street, Chicago, IL 60637, USA

E-mail: cowan@math.uchicago.edu, jneuman@uchicago.edu, b.kiewiet-1@student.utwente.nl and wvandron@peds.bsd.uchicago.edu

Received 15 September 2012

Accepted 25 March 2013

Published 26 April 2013

Online at stacks.iop.org/JSTAT/2013/P04030

doi:[10.1088/1742-5468/2013/04/P04030](https://doi.org/10.1088/1742-5468/2013/04/P04030)

Abstract. This paper contains an analysis of a simple neural network that exhibits self-organized criticality. Such criticality follows from the combination of a simple neural network with an excitatory feedback loop that generates bistability, in combination with an anti-Hebbian synapse in its input pathway. Using the methods of statistical field theory, we show how one can formulate the stochastic dynamics of such a network as the action of a path integral, which we then investigate using renormalization group methods. The results indicate that the network exhibits hysteresis in switching back and forward between its two stable states, each of which loses its stability at a saddle-node bifurcation. The renormalization group analysis shows that the fluctuations in the neighborhood of such bifurcations have the signature of directed percolation. Thus, the network states undergo the neural analog of a phase transition in the universality class of directed percolation. The network replicates the behavior of the original sand-pile model of Bak, Tang and Wiesenfeld in that the fluctuations about the two states show power-law statistics.

Keywords: renormalization group, phase transitions into absorbing states (theory), self-organized criticality (theory), neuronal networks (theory)

ArXiv ePrint: [1209.3829](https://arxiv.org/abs/1209.3829)

Contents

1. Introduction	3
1.1. Criticality in neural activity	3
1.2. Self-organized criticality	4
1.3. The mechanism of SOC	4
2. Neural network dynamics	4
2.1. Annihilation and creation operators	6
2.2. A neural state vector and expectation values.	7
2.3. A neural master equation	8
2.4. From bosons to coherent states	8
2.5. The continuum limit of \mathcal{H}	9
2.6. Dimensions and the density representation	9
2.7. From the quasi-Hamiltonian to a neural path integral.	10
3. The dynamics of synaptic plasticity	10
3.1. Developing an action for synaptic plasticity	11
4. Combining the actions	13
4.1. A simulation of the behavior of the combined mean-field equations	13
4.2. Renormalizing the combined action.	13
4.2.1. Renormalizing the neural action.	14
4.2.2. Renormalizing the driven neural action.	16
4.2.3. Renormalizing the synaptic plasticity action.	16
4.2.4. Renormalizing the combined action.	16
5. Simulating the effects of fluctuations	16
6. Discussion	18
Acknowledgments	19
Appendix	19
A.1. Expanding the weighting function.	19
A.2. Renormalizing the neural action.	20
A.3. Renormalizing the synaptic plasticity action	22
A.4. Renormalizing the driven neural action.	23
A.5. Renormalizing the combined action.	23
References	23

1. Introduction

There is no question that the analysis of large-scale brain activity is a very hard problem. There are approximately 50 billion neurons in the human cortex, of which 80% are excitatory, and the remaining 20% are inhibitory. Each neuron has about four thousand axon terminals from other neurons, but because of the redundancy of axon terminal arbors it has effective connections from about 50 other neurons. In the simplest model, neurons are binary switches, either *quiescent* or *activated*. Therefore, there are approximately $10^{1.5 \times 10^{10}}$ configurations. Such a large configuration space suggests the need to use statistical methods to analyze large-scale brain activity. The appearance of microscopic randomness in cortical connectivity, and of intrinsic fluctuations in cortical activity, further reinforces this conclusion. Such considerations led initially to the mean-field equations for a spatially homogeneous population of coupled excitatory and inhibitory neurons [39], and their extension to the spatially inhomogeneous case [40]. However, this analysis, being mean-field, is unable to deal with the effects of microscopic randomness, or intrinsic fluctuations and correlations. This led one of us (JDC) to formulate a fully stochastic treatment of large-scale brain activity, during the late 1970s. This effort led ultimately to the work reported in [9]. In this paper we used modern methods of statistical mechanics and field theory, including renormalization group methods, to study the possibility of phase transitions in large-scale brain activity, and the associated phenomena associated with critical behavior.

1.1. Criticality in neural activity

There is now a considerable amount of literature on criticality in brain activity, much of it speculative. However, there is one solid piece of data obtained by Beggs and Plenz [7] in a study of spontaneous activity in an isolated slab of cortical tissue. Beggs and Plenz followed up a much earlier series of experiments on isolated cortical slabs or slices carried out by Burns [15]. His main result was that an isolated cortical slab remains silent but excitable by brief current pulses. A strong enough pulse can trigger a sustained all-or-none response that propagates radially from the stimulation site, at a velocity of about 15 cm s^{-1} . From this, Burns concluded that the slab had become epileptic, and noted that behind the radially propagating front the activity consisted of random bursts of spikes.

However, Burns did not study the effects of near-threshold stimuli, nor did he use an array of electrodes, as Beggs and Plenz did 50 years later. They stimulated slabs with a mixture of NMDA, a glutamate receptor agonist, and a dopamine D_1 receptor agonist, and found using an 8×8 electrode array that the slabs became spontaneously active, generating random bursts of spike activity. An analysis of such bursts indicated that their statistical properties were time-scale invariant, i.e. *self-similar*, and could be described as *avalanches*. In addition, the distribution of such avalanches was the power-law $P(n) \propto n^{-\alpha}$, where n is the avalanche size (equal to the number of activated electrodes in the array) and $\alpha = -3/2$. This power-law is a signature of *mean-field critical branching* [4], which led Beggs and Plenz to posit that the statistical dynamics of the spontaneous slab activity exhibits criticality.

This raises two questions. The first question is what kind of neural population dynamics can exhibit branching behavior, in particular critical branching behavior? The second question is if a neural population does exhibit such behavior, does it need to be tuned externally, or is it self-tuning? The first question was answered by Buice and Cowan [9], who showed that a single population of spatially coupled excitatory neurons could be tuned to exhibit spontaneous activity in the form of bursts of spikes, and that the statistical dynamics of the network could be represented as the action of a Wiener path integral. Remarkably, the renormalized form of this action is that of Reggeon field theory [3] (see also [14]). We describe a slightly reformulated version of this work in what follows. An answer to the second question constitutes the main part of this paper.

1.2. Self-organized criticality

We first restate the second question as that of the possible existence of self-organized criticality (SOC) in large-scale brain activity. The idea of self-organized criticality (SOC) was introduced by Bak *et al* [6]. Their paper immediately triggered an avalanche of papers on the topic, including many on brain dynamics, in which it was claimed that the mere presence of power-law scaling in neocortical dynamics is evidence of criticality, especially SOC (see the review by Buice and Cowan [10]). Here, we present a very simple model of a neural circuit with a modifiable synapse in which we can demonstrate the existence of SOC, not only by simulation, but also by a detailed analysis of both the mean-field and stochastic dynamics of the circuit, using statistical field theory, including the renormalization group method.

1.3. The mechanism of SOC

Our starting point is the paper by Gil and Sornette [17], which contains a clear analysis of the essential requirements for SOC: (1) an *order-parameter* equation for a dynamical system with a time-constant τ_o , with stable equilibria separated by a threshold, (2) a *control-parameter* equation with a time-constant τ_c , and (3) a steady *driving force*. In Bak *et al*'s classic example, the sand-pile model, the order parameter is the flux of sand grains down a sand-pile, the control parameter is the sand-pile's slope, and the driving force is a steady flow of grains of sand onto the top of the pile. Gil and Sornette showed that if $\tau_o \gg \tau_c$ then the resulting avalanches of sand down the pile would have a scale-free distribution, whereas if $\tau_o \ll \tau_c$ then the distribution would also exhibit one or more large avalanches.

In this paper we will analyze a neural network model in which neural network activity is the order parameter, and the strength of a modifiable synapse in the input pathway to the network is the control parameter. Such a setup is in one-to-one correspondence with the Gil-Sornette SOC-model, and therefore should also exhibit SOC.

2. Neural network dynamics

Consider first the mathematical representation of the dynamics of a neocortical slab comprising a single population of N excitatory neurons. Such neurons make transitions from an inactivated or quiescent state q to an activated state a at the rate f , and back again to the state q at the rate α , as shown in figure 1. The configuration space of the population

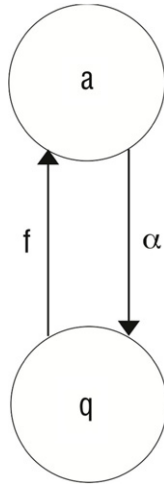


Figure 1. Neural state transitions. a is the activated state of a neuron, q is the inactivated or quiescent state, α is a constant, but f depends on the number of activated neurons connected to the i th neuron, and (possibly) an external stimulus h .

is that of distinguishable patterns of neural activity defined by the states a and q . There are 2^N such patterns, and since $N \approx 5 \times 10^{10}$, the space is large. There are undoubtedly many sources of noise in neural activity, so that a statistical description of this activity is required. Consider therefore the probability distribution $P(\nu_1, \nu_2, \dots, \nu_N, t) = P(\boldsymbol{\nu}, t)$, where $\nu_i = 1$ if the i th neuron is activated at time t , and $\nu_i = 0$ if it is quiescent at time t . We need to derive a *master equation* for the evolution of $P(\boldsymbol{\nu}, t)$.

We first consider all the state transitions that can occur in an asynchronous noisy network of N excitatory neurons. Let A be the total number of activated neurons in the network at time t , and $Q = N - A$ be the total number of quiescent neurons at time t . The possible transitions that can occur in the network comprise $A \rightarrow A$ (no change), $A - 1 \rightarrow A$ (a quiescent neuron becomes active at the rate f), and $A \rightarrow A - 1$ (an activated neuron becomes quiescent at the rate α).

The rate function $f = f[s(I_i)]$ represents the transition from a quiescent to an activated neuron at the i th site, at the rate $f[s(I_i)]$, where

$$s(I_i) = k_i I_i = \frac{1}{I_{\text{RH},i}} \left(\sum_j w_{ij} n_j + h_i \right), \quad k_i = \frac{1}{I_{\text{RH},i}} \quad (1)$$

is the current to the i th neuron, $I_{\text{RH},i}$ is its threshold or *rheobase* current, w_{ij} is the weight of the synapse between the j th and i th neurons, n_j represents an activated neuron at the j th site and h_i represents an external spike stimulating the i th neuron.

The transition rate $f[s(I)]$ is shown in figure 2. It is essentially the integral of

$$\int_{-\infty}^{I_{\text{RH}}} P(\theta) d\theta$$

where $P(\theta)$ is the probability distribution of threshold currents in the neural population. We note that such a function has $f^{(1)} > 0$, $f^{(2)} < 0$ above its inflection point, and, therefore,

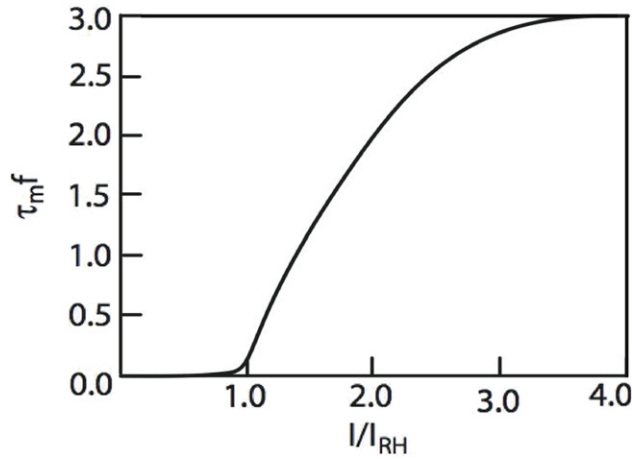


Figure 2. Graph of the firing rate function $f[s(I)]$. $\tau_m = 1/\alpha = 3$ is the membrane time-constant (in ms). $s(I) = I/I_{\text{TH}}$ is the input current, where $I_{\text{TH}} \equiv I_{\text{RH}}$ is the threshold or *rheobase* current.

after appropriate translations of the axes [39], supports the possibility of bistability in the neural dynamics.

Let $N = 1$ and $P(1, t)$ be the probability that such a neuron is activated, and $P(0, t)$ that it is quiescent. The resulting master equation takes the simple form

$$\frac{dP(1, t)}{dt} = -\alpha P(1, t) + f[s]P(0, t). \quad (2)$$

We need to extend such a master equation to deal with the full network of N neurons generating 2^N configurations, and therefore 2^N simultaneous equations. We follow [14], [9], and [10] and introduce an operator representation for the required master equation, in the style of quantum field theory. However, we modify the derivation somewhat and introduce a microscopic condition that limits the occupancy of the i th site to $\nu_i = 1$ or else 0 as required.

2.1. Annihilation and creation operators

We begin by defining an $N = 0$ network vector to be

$$|\text{network with 0 neurons}\rangle = |0\rangle. \quad (3)$$

We next introduce Fock space *annihilation* and *creation* operators satisfying boson commutation rules

$$\begin{aligned} [a_i, a_j^\dagger] &= [q_i, q_j^\dagger] = \delta_{ij} \\ [a_i, a_j] &= [a_i^\dagger, a_j^\dagger] = 0 \\ [q_i, q_j] &= [q_i^\dagger, q_j^\dagger] = 0. \end{aligned} \quad (4)$$

Such operators act on a state vector $|n_i\rangle$ representing n_i activated neurons at the i th site, and its dual, so that

$$\begin{aligned} a_i^\dagger |n_i\rangle &= |n_i + 1\rangle, & a |n_i\rangle &= n_i |n_i - 1\rangle \\ \langle n_i | a_i^\dagger &= \langle n_i - 1 | n_i, & \langle n_i | a &= \langle n_i + 1 |. \end{aligned} \quad (5)$$

These operate on the *vacuum* vector $|0\rangle$ to generate vectors comprising activated or quiescent neurons. The configuration space vector $|\nu\rangle$ is thus generated as

$$|\nu\rangle = \prod_{i=1}^{2^N} \Phi_{\nu_i}^\dagger |0\rangle \quad (6)$$

where

$$\Phi_{\nu_i}^\dagger = \begin{cases} a_i^\dagger & \text{if } \nu_i = 1 \\ q_i^\dagger & \text{if } \nu_i = 0 \end{cases} \quad (7)$$

and the dual configuration space vector $\langle\nu|$ is generated as

$$\langle\nu| = \prod_{i=1}^{2^N} \langle 0| \Phi_{\nu_i} \quad (8)$$

where

$$\Phi_{\nu_i} = \begin{cases} a_i & \text{if } \nu_i = 1 \\ q_i & \text{if } \nu_i = 0. \end{cases} \quad (9)$$

Inner products in the resulting vector space are generated by $\langle 0|0\rangle = 1$ and the commutation relations in equation (4).

2.2. A neural state vector and expectation values

We now define a network state vector as the weighted sum over all configurations, where the weight is the probability distribution given in the master equation,

$$|\phi(t)\rangle = \sum_{\nu} P(\nu, t) |\nu\rangle. \quad (10)$$

Let

$$|p\rangle = \exp\left(\sum_{i=1}^N a_i^\dagger\right) |0\rangle. \quad (11)$$

If we apply the dual vector $\langle p|$ to the state $|\phi(t)\rangle$ we obtain

$$\langle p|\phi(t)\rangle = \sum_{\nu} P(\nu) = 1, \quad \text{and} \quad \langle p|\partial_t|\phi(t)\rangle = -\langle p|\hat{H}|\phi(t)\rangle = 0$$

which is probability conservation.

We note that applying the operator $a_i^\dagger a_i$ to the configuration vector $|\nu\rangle$ asks the question is the i th neuron activated? If the answer is positive the operator leaves the i th state untouched, if negative the answer is 0. Thus, the operator $\sum_i a_i^\dagger a_i$ counts the number of activated neurons in $|\nu\rangle$. Similarly, the operator $\sum_i q_i^\dagger q_i$ counts the number of quiescent neurons in $|\nu\rangle$.

We can use the projection technique to calculate the expected number of activated neurons at the i th site using the number operator $a_i^\dagger a_i$. Let p_i be the probability that the i th neuron is activated. Then

$$\langle p|a_i^\dagger a_i|\phi(t)\rangle = \sum_{\nu} n_i P(\nu) = \langle n_i \rangle = p_i. \quad (12)$$

In similar fashion

$$\langle p | a_i^\dagger a_i a_j^\dagger a_j | \phi(t) \rangle = \sum_{\nu} n_i n_j P(\nu) = \langle n_i n_j \rangle = p_{ij}. \quad (13)$$

In the model considered here n_i and n_j are restricted to the values 0 and 1. This restriction is achieved using the microscopic occupancy condition,

$$a_i^\dagger a_i + q_i^\dagger q_i = 1. \quad (14)$$

All configurations in the vector space $|\nu\rangle$ are thus restricted, and are called *physical* states.

Finally, we note that we can use the commutation rules introduced in equation (4) to commute $\exp(\sum_i a_i^\dagger)$ all the way to the right in expectation values, so that they take the form of a *vacuum expectation* value $\langle A \rangle = \langle 0 | A | 0 \rangle$. It can be shown that this is equivalent to the shift $a_i^\dagger \rightarrow a_i^\dagger + 1$, so that $a_i^\dagger a_i \rightarrow a_i^\dagger a_i + a_i$. We will employ this shift shortly.

2.3. A neural master equation

We now construct a neural master equation using the operators introduced above, as

$$\frac{d}{dt} |\phi(t)\rangle = \sum_i \left[\alpha (1 - a_i^\dagger) a_i + (a_i^\dagger - 1) (1 - a_i^\dagger a_i) f[s(I_i)] \right] |\phi(t)\rangle \quad (15)$$

or formally as

$$\frac{d}{dt} |\phi(t)\rangle = -\hat{H} |\phi(t)\rangle \quad (16)$$

where

$$-\hat{H} = \sum_i \left[\alpha (1 - a_i^\dagger) a_i + (a_i^\dagger - 1) (1 - a_i^\dagger a_i) f[s(I_i)] \right] \quad (17)$$

is the *quasi-Hamiltonian* operator.

This operator is constructed by noting that

$$\left[\alpha (1 - a_i^\dagger) a_i + (a_i^\dagger - 1) (1 - a_i^\dagger a_i) f[s(I_i)] \right] |\nu_i\rangle \quad (18)$$

only gives a non-zero contribution from the first term when $\nu_i = 1$ and a contribution from the second term when $\nu_i = 0$. Thus it correctly represents the transitions between quiescent and active in the neuron at the site i , and the factor $1 - a_i^\dagger a_i = q_i^\dagger q_i$ eliminates the q -state variable from the expression, by using equation (14) to limit occupancy at the site i to one state. (See [35] and [33].)

2.4. From bosons to coherent states

Equation (16) is a linear operator equation with formal solution

$$|\phi(t)\rangle = \exp \left[-\hat{H}(t - t_0) \right] |\phi(t_0)\rangle.$$

We need to re-express this solution in terms of complex numbers rather than operators. This can be achieved by introducing *coherent states*. These were introduced by Schrödinger [31] and first used extensively in coherent optics by Glauber [19]. We therefore introduce

such states $|\varphi_i\rangle$ in the form

$$|\varphi_i\rangle = \exp[-\frac{1}{2}\varphi_i^* \varphi_i + \varphi_i a_i^\dagger] |0_i\rangle \quad (19)$$

where φ_i is the right eigenvalue of a_i , i.e. $a_i|\phi_i\rangle = \varphi_i|\phi_i\rangle$. There is also a coherent state representation of q_i in the form $|\vartheta_i\rangle$ such that the right eigenvalue of q_i is ϑ_i , i.e. $q_i|\vartheta_i\rangle = \vartheta_i|\vartheta_i\rangle$. In similar fashion $\langle\varphi_i|a_i^\dagger = \langle\varphi_i|\tilde{\varphi}_i$, where $\tilde{\varphi}_i$, the complex conjugate of φ_i , is the left eigenvalue of a_i^\dagger , and similarly $\langle\vartheta_i|q_i^\dagger = \langle\vartheta_i|\tilde{\vartheta}_i$, i.e. $\tilde{\vartheta}_i$ is the left eigenvalue of q_i^\dagger . It follows that

$$\langle\varphi_i|a_i^\dagger a_i|\varphi_i\rangle = \langle\varphi_i|\tilde{\varphi}_i\varphi_i|\varphi_i\rangle = \tilde{\varphi}_i\varphi_i. \quad (20)$$

All this suggests that the operator quasi-Hamiltonian has a coherent state representation in the form

$$-\mathcal{H} = \sum_i [\alpha(1 - \tilde{\varphi}_i)\varphi_i + (\tilde{\varphi}_i - 1)(1 - \tilde{\varphi}_i\varphi_i)f[s(I_i)]] \quad (21)$$

where

$$s(I_i) \propto \sum_j w_{ij}\tilde{\varphi}_j\varphi_j + \tilde{h}_i h_i. \quad (22)$$

We note that in transforming to the coherent state representation we must again use the commutation rules to ensure that all creation operators a_i^\dagger precede the annihilation operators a_i , to produce the *normal ordered* form. Thus, the normal ordered form of $a_i^\dagger a_i a_i^\dagger$ is written as $:a_i^\dagger a_i a_i^\dagger := (a_i^\dagger)^2 a_i + a_i^\dagger$. It follows from this that we need to expand the function $f[s(a^\dagger, a)]$ in powers of $s(a^\dagger, a)$ in order to produce the normal ordered form of \mathcal{H} . We do this in appendix, but will defer including the results in the main body of the paper until later.

2.5. The continuum limit of \mathcal{H}

The final preliminary step of this formulation is to take the *continuum limit* of the expression for \mathcal{H} in equation (21), so that

$$\mathcal{H} = \int d^d x [\alpha\tilde{\varphi}\varphi - \tilde{\varphi}(\rho - \tilde{\varphi}\varphi - \varphi)f[s(\tilde{\varphi}\varphi + \varphi)]] \quad (23)$$

in which $\varphi_i \rightarrow \rho\varphi(\mathbf{x}, t) \equiv \varphi$ etc, where ρ is the packing density of neurons in the neocortex, and the conjugate coherent state $\tilde{\varphi}$ has been shifted to $\tilde{\varphi} + 1$.

Note that in taking the continuum limit we make the assumption that the cortex is translation symmetric on the relevant length scales of mm to cm. This requires that we assume that $w_{ij} \rightarrow w_{i-j}$, so that in the continuum limit $w_{ij} \rightarrow w(\mathbf{x} - \mathbf{x}')$ and $\sum_j w_{ij} \rightarrow w \star$, where \star is the convolution operator $\int d^d x' w(\mathbf{x} - \mathbf{x}')$.

2.6. Dimensions and the density representation

Before proceeding further we need to assign a dimension to each variable in equation (23). To do so we use a modified version of the convention used in particle physics so that $[x] = L^{-1}$, $[t] = L^{-2}$, where L is the length scale used, whence $[x^2/t] = L^0$. (This generates a scaling found in Markov random walks and related processes such as stochastic neural

activity.) Then, $[\alpha] = L^2$, $[\varphi] = L^d$, $[\tilde{\varphi}] = L^0$, $[\tilde{\varphi}\varphi] = L^d$, $[f[s]] = [\alpha] = L^2$. This last value of $[f[s]]$ implies that the input current function $s(\tilde{\varphi}\varphi + \varphi) = s(I) = kI$, where the constant k has the dimensions of inverse current density, so that $[s] = L^0$. The net effect of such a choice leads to the required result that $[\mathcal{H}] = 2$.

To emphasize this choice we further transform the coherent state quasi-Hamiltonian by introducing the *density representation*,

$$\tilde{\varphi} + 1 \rightarrow e^{\tilde{n}}, \quad \varphi \rightarrow ne^{-\tilde{n}} \quad (24)$$

where $n(\mathbf{x}, t)$ is the local density of activated neurons. Then, equation (23) transforms into

$$\mathcal{H} = \int d^d x [\alpha(1 - \exp(-\tilde{n}))n - (\exp \tilde{n} - 1)(\rho - n)f[s(w \star n + h)]]. \quad (25)$$

2.7. From the quasi-Hamiltonian to a neural path integral

Using standard methods [16, 30], Buice and Cowan [9] incorporated the quasi-Hamiltonian into the action of a Wiener path integral. This action takes the form

$$S(n) = \iint d^d x dt [\tilde{n}\partial_t n + \alpha(1 - e^{-\tilde{n}})n - (e^{\tilde{n}} - 1)(\rho - n)f[s(w \star n + h)]]. \quad (26)$$

The significance of this action is that it can be used to construct a generating functional for statistical moments of the probability density $P[\nu, t]$ such as the mean spike count at the location \mathbf{x} at the instant t , $\langle n(\mathbf{x}, t) \rangle$, and the correlation function $\langle n(\mathbf{x}, t)\tilde{n}(\mathbf{x}', t') \rangle$, etc.

This generating functional is the path integral

$$\mathbb{Z}[\tilde{J}(\mathbf{x}, t), J(\mathbf{x}, t)] = \iint \mathcal{D}n\mathcal{D}\tilde{n} e^{-S(n, \tilde{n}) + \tilde{J} \cdot n + J \cdot \tilde{n}} \equiv \left\langle \exp[\tilde{J} \cdot n + J \cdot \tilde{n}] \right\rangle \quad (27)$$

where $\mathcal{D}n\mathcal{D}\tilde{n}$ is the Wiener measure, and $\tilde{J} \cdot n = \int d^d x \tilde{J}(\mathbf{x}, t)n(\mathbf{x}, t)$, etc. Functional differentiation of this and related expressions w.r.t. J and \tilde{J} , subject to the conditions $J, \tilde{J} = 0$, generates the various moments and moment equations. In particular, we obtain the first moment or mean-field Wilson–Cowan equations [40],

$$\partial_t \langle n \rangle = -\alpha \langle n \rangle + (\rho - \langle n \rangle)f[s(w \star \langle n \rangle + \langle h \rangle)]. \quad (28)$$

Thus, the Wilson–Cowan equation is a nonlinear integro-differential equation. The derivation given here presents one way to extend these equations to a stochastic formulation that can be analyzed by the techniques of statistical field theory.

We further note that if the population activity is sparse, then $\rho - n \rightarrow \rho$ in equation (26) and $1 - a_i^\dagger a_i \rightarrow 1$ in equation (17). These equations then become, respectively, the action and master equations for the *spiking* model described in [9] and [10], except that n_i is now interpreted as the number of spikes emitted by the i th neuron.

3. The dynamics of synaptic plasticity

We now turn to the mathematical representation of synaptic plasticity and consider first a single excitatory neuron e_i embedded in a network E of excitatory neurons. Such a neuron receives input currents from neurons in the network, and also from a population

H of other neurons outside the network. Equation (1) now reads

$$s(I_i) = k_i \left(\sum_j w_{ij}^E n_j + \sum_k w_{ik}^H n_k \right). \quad (29)$$

We now consider a single input n'_k from H , acting on e_i through the synapse w_{ik}^H . We can implement this by letting $w_{ik}^H \rightarrow w_{ik}^H \delta_{kk'}$, so that $\sum_k w_{ik}^H n_k \rightarrow w_{ik'} n'_k$. The continuum limit of the expression for the current from H therefore takes the form:

$$\int d^d x' w_H(\mathbf{x}, \mathbf{x}') n_H(\mathbf{x}') \rightarrow \int d^d x' b_H(\mathbf{x}, \mathbf{x}') \delta^d(\mathbf{x} - \mathbf{x}') n_H(\mathbf{x}') = b_H(\mathbf{x}) n_H(\mathbf{x}). \quad (30)$$

The synaptic weight $b_H(\mathbf{x})$ is *modifiable*, Its mean-field equation takes the form

$$\frac{d\langle b_H(\mathbf{x}) \rangle}{dt} = -\beta g_E(\mathbf{x}) \left(\frac{\langle n_E(\mathbf{x}) \rangle}{\rho_S} - \frac{\langle n_{E,0}(\mathbf{x}) \rangle}{\rho_S} - \kappa_{E,S} \langle b_H(\mathbf{x}) \rangle \right) \frac{\langle n_H(\mathbf{x}) \rangle}{\rho_S} \quad (31)$$

where β is the rate constant for weight changes, ρ_S is the density of synapses at \mathbf{x} , and g_E is the state-dependent function,

$$g_E(\mathbf{x}) \approx \frac{k(\mathbf{x}) F'}{1/\rho - k(\mathbf{x}) F' w_0} \quad (32)$$

where $F = f/(\alpha + f)$, $\langle n_{E,0}(\mathbf{x}) \rangle$ is a constant neural activity, w_0 is the total synaptic weight per neuron (see appendix), and $\kappa_{E,S} = L(0) < 0$ is a constant derived from the *window function* $L(\Delta t)$ of spike-time dependent plasticity (STDP) used in [36]. The ratios $\langle n_E(\mathbf{x}) \rangle / \rho_S$, $\langle n_{E,0}(\mathbf{x}) \rangle / \rho_S$, $\langle n_H(\mathbf{x}) \rangle / \rho_S$ have dimension L^0 , and represent *mean numbers of spikes*. The expression for $g_E(\mathbf{x})$ is approximate in the sense that for values of the rate constant $\alpha \ll \beta$ it requires corrections that are hard to calculate. However, most of our simulations are not in such a range.

In equation (31) the synaptic weight $b_H(\mathbf{x})$ is depressed by an *anti-Hebbian* mechanism, and potentiated by the input activity n_H . Such an equation was first introduced in [36] for a purely feedforward circuit with no loops, and a linear firing rate function f , in which the synapse was inhibitory rather than excitatory, and Hebbian rather than anti-Hebbian. The Vogels formulation has an important property: the equation can be shown to implement gradient descent to find the minimum of an energy function, the effect of which is to balance incoming excitatory and inhibitory currents to the output neuron. Equation (31) is an extension of the Vogels equation to the case of circuits with feedback loops, and a nonlinear firing rate function f , and incorporates modifiable synapses that are excitatory and anti-Hebbian. In fact there is experimental evidence to support both kinds of synapses [23, 37]. It remains to formulate an action for the master equation that generates this mean-field equation.

3.1. Developing an action for synaptic plasticity

To derive an action for synaptic plasticity we follow the same procedure as before. We first formulate the changes in b_H as a Markov process with discrete states in continuous time. We therefore assume that b_H is *quantized* in units of synaptic weight, and similarly for b_E . (Note: we could formulate the changes in b_H as a Markov process with continuous

states and use duality to obtain a bosonic action for a discrete state Markov process [29]. Here we proceed in the opposite direction.)

We first introduce bosonic annihilation and creation operators for b_{ik}^H . Let such operators be denoted by b_{ik}^\dagger and b_{ik} respectively, and let $|b_{ik}^H\rangle$ be a column vector representing the synaptic weight b_{ik}^H such that

$$b_{ik}^\dagger |b_{ik}^H\rangle = |b_{ik}^H + 1\rangle, \quad b_{ik} |b_{ik}^H\rangle = b_{ik}^H |b_{ik}^H - 1\rangle. \quad (33)$$

Such operators act on a configuration space built from a null synapse, i.e. a synapse with weight $b_{ik}^H = 0$. Let this be represented, again, by the vacuum vector $|0\rangle$. The configuration space vector $|\zeta\rangle$ then ranges from $b_{ik}^H = 0$ to $b_{ik}^H = (b_{ik}^H)_{\text{MAX}} = M_i$, where M_i is the maximum synaptic weight per neuron, which is a limit imposed by the finite surface area of any individual neuron's membrane. Let S be the number of (effective) synapses per neuron. Then

$$|\zeta\rangle = \prod_{i=1}^N \prod_{k=1}^S (b_{ik}^H)^\dagger |0\rangle. \quad (34)$$

The dual vector $\langle\zeta|$ can be defined in similar fashion, and a synaptic state vector

$$|\theta(t)\rangle = \sum_{\zeta} P(\zeta, t) |\zeta\rangle \quad (35)$$

can be introduced. The rest of the development (almost) completely parallels that for neural activity introduced earlier.

We next look at the steps necessary to construct a quasi-Hamiltonian for synaptic plasticity. The first thing to do is to model the synaptic state transitions $b_{ik}^H + 1 \rightarrow b_{ik}^H$ and $b_{ik}^H \rightarrow b_{ik}^H + 1$ as a Markov process. Following the formulation of the neural quasi-Hamiltonian in equation (18) we construct a provisional synaptic quasi-Hamiltonian in the form

$$- \hat{H}_b = \sum_i \left[\lambda (1 - b_{ik'}^\dagger) b_{ik'} + \mu (b_{ik'}^\dagger - 1) \right] \quad (36)$$

where λ and μ are state-dependent rate functions. Comparison with equation (31) indicates that we require

$$\lambda = \beta g_{E,i} |\kappa_{E,S}| \frac{n_{H,k'}}{\rho_S}, \quad \mu = \beta g_{E,i} \frac{(n_{E,0,i} - n_{E,i}) n_{H,k'}}{\rho_S \rho_S} \quad (37)$$

to correctly generate the mean-field equation.

Thus, we can write the quasi-Hamiltonian in the form

$$- \hat{H}_b = \sum_i \left[\beta g_{E,i} |\kappa_{E,S}| \frac{n_{H,k'}}{\rho_S} (1 - b_{ik'}^\dagger) b_{ik'} + \beta g_{E,i} \frac{(n_{E,0,i} - n_{E,i}) n_{H,k'}}{\rho_S \rho_S} (b_{ik'}^\dagger - 1) \right]. \quad (38)$$

We note an important difference between this \hat{H}_b and the neural quasi-Hamiltonian \hat{H} , apart from the fact that they work on different configuration spaces. There is no restricted occupancy condition in \hat{H}_b , and it is now a simple matter to introduce a coherent state representation of \hat{H}_b , shift to the density representation and construct the action for synaptic plasticity $S(b_H)$, and take the continuum limit. The result is

$$S(b_H) = \iint d^d x dt \left[\tilde{b}_H \partial_t b_H + \beta g_E |\kappa_{E,S}| \frac{n_H}{\rho_S} (1 - e^{-\tilde{b}_H}) b_H - \beta g_E (n_{E,0} - n_E) \frac{n_H}{\rho_S} (e^{\tilde{b}_H} - 1) \right] \quad (39)$$

where $b_H \rightarrow \rho_S b_H = b_H(\mathbf{x})$, a *weight density*, $g_{E,i} \rightarrow g_E(\mathbf{x})$, etc. Using variational techniques we can derive equation (31) from $S(b_H)$.

4. Combining the actions

It follows from this formulation that the full action for the coupled system of equations for the evolution of n_E and b_H can be obtained simply by adding the actions $S(n_E)$ and $S(b_H)$ together. The combined action therefore takes the form

$$S(n_E, b_H) = \iint d^d x dt \left[\tilde{n}_E \partial_t n_E + \alpha(1 - e^{-\tilde{n}_E}) n_E - (e^{\tilde{n}_E} - 1)(\rho - n) f[s(n_E)] \right. \\ \left. + \tilde{b}_H \partial_t b_H + \beta g_E |\kappa_{E,S}| \frac{n_H}{\rho_S} (1 - e^{-\tilde{b}_H}) b_H - \beta g_E (n_{E,0} - n_E) \frac{n_H}{\rho_S} (e^{\tilde{b}_H} - 1) \right] \quad (40)$$

where the current $s(n_E) = k(w \star n_E + b_H \delta^d \star n_H)$. Note that the time scale of the growth and decay of neural activity is set by the constant α , whereas that of the growth and decay of synaptic plasticity is set by βg_E , which is both state and position dependent. Thus the ratio $\alpha/\beta g_E$ is an important parameter.

4.1. A simulation of the behavior of the combined mean-field equations

The first variation of equation (40) generates the mean-field equations for n_E and b_H in the form

$$\frac{\partial_t \langle n \rangle}{\partial t} = -\alpha \langle n \rangle + (\rho - \langle n \rangle) f[s(\langle I_E \rangle)] \quad (41) \\ \frac{\partial \langle b_H(\mathbf{x}) \rangle}{\partial t} = -\beta g_E (\langle n_E(\mathbf{x}) \rangle - \langle n_{E,0}(\mathbf{x}) \rangle - \kappa_{E,S} \langle b_H(\mathbf{x}) \rangle) \frac{\langle n_H(\mathbf{x}) \rangle}{\rho_S}$$

where

$$s_E(\langle I_E \rangle) = k(w_E \star \langle n_E \rangle + \langle b_H \rangle \langle n_H \rangle). \quad (42)$$

These equations can be simulated. The results are shown in figure 3. It will be seen that in the ‘ground-state’ of low values of $N^* = n_E^*$ the synaptic weight b_H increases until it reaches a critical point (a saddle–node bifurcation), at which point N^* becomes unstable and the system switches to the ‘excited-state’. But then the anti-Hebbian term in the synaptic plasticity dynamics kicks in, and b_H declines until the excited-state fixed-point becomes unstable at the upper critical point, (also a saddle–node bifurcation), and switches back to the ground-state fixed point, following which the hysteresis cycle starts over. This is an exact representation of the sand-pile model’s behavior. The reader should compare this with the synaptic mechanisms described in [25] and in [26].

4.2. Renormalizing the combined action

The mean-field behavior we have described fits the Bak *et al* setup for achieving SOC very well. However, such an analysis does not account for the effects of fluctuations. We need the stochastic formulation for such a project. There are two situations to consider: (a) when the fixed point values N^* of the neural activity are stable, and (b) when N^* becomes

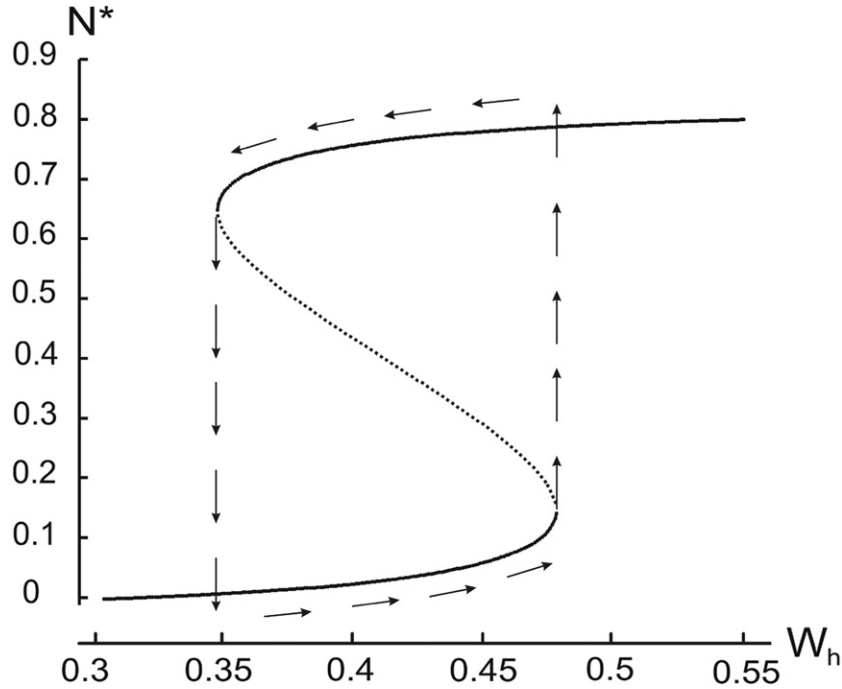


Figure 3. Neural state transitions between a ground state and an excited state. Parameter values: $m_E = 3, n_H = 3; \alpha = 0.2$. N^* is the fixed-point value of n_E , and W_H is the magnitude of the anti-Hebbian synapse in the input path.

marginally stable. In case (a) we can use the van Kampen system-size expansion [34] to develop a linear Fokker–Planck equation, and its associated linear Langevin equation to describe the fluctuations about N^* . The reader is referred to [8] for an example of such a treatment in a network comprising coupled excitatory and inhibitory neurons.

4.2.1. Renormalizing the neural action. However, case (b) requires a renormalization group treatment. All the details of such a treatment are described in appendix. We first renormalize the neural action given in equation (40) in the case where the external stimulus $n_H = 0$, so that the resulting spontaneous activity is driven only by internal fluctuations.

The result is

$$S(s_E) = \iint d^d x dt [\tilde{s}_E(\partial_t + \mu_E - D_E \nabla^2)s_E + u_E \tilde{s}_E(s_E - \tilde{s}_E)s_E]. \quad (43)$$

This action is well-known: it is called Reggeon field theory, and is found in directed percolation (DP) in random graphs, in contact processes, in high-energy nuclear physics, and in bacterial colonies, all of which exhibit the characteristic properties of what is called a *universality class*, i.e., it is a phase transition with a universal scaling of important statistical exponents. It also shows up in branching and annihilating random walks, catalytic reactions, and interacting particles. Thus, we have mapped the mathematics of large-scale neural activity in a single homogeneous neural population into a percolation problem in random graphs, or equivalently into a branching and annihilating random walk. A first version of this work was presented in [9]. A more extensive paper with many applications to neuroscience was presented in [10].

Note that \tilde{s}_E and s_E are scaled versions of \tilde{n}_E and n_E , where the latter is no longer interpreted to be the density of activated neurons at a given location, but the *fluctuation* in n_E about the mean value $\langle n_E \rangle = n_{E,cl}$, as detailed in section A.2.

It is also important to note that in DP there are essentially two stable states separated by a marginally stable critical point. One of these states is an *absorbing* state, corresponding to a neural population state in which all neurons are quiescent, $\langle n \rangle = 0$ (e.g. they are all subject to an inhibitory or *hyperpolarizing* current), or a sub-threshold excitatory current. The other state is one in which many of the neurons are activated, so that $\langle n \rangle \neq 0$, i.e. the order parameter is zero in the lower stable state, and is non-zero in the upper stable state. At a critical point (corresponding to a saddle–node bifurcation in the mean-field analysis), the lower state with $\langle n \rangle = 0$ becomes marginally stable, and so is driven by fluctuations into the upper stable state.

Here, we note that there is an *upper critical dimension* at which directed percolation crosses over to mean-field behavior. This upper critical dimension is $d = 4$. What is the dimension of the neocortex? To answer this question we note that the neocortex can be unfolded and flattened into a slab with the dimensions $1 \text{ m} \times 1 \text{ m} \times 3 \text{ mm} = 3 \times 10^6 \text{ mm}^3$. Since there are an estimated 5×10^{10} neurons in the neocortex, their packing density is $\rho = 1.67 \times 10^4 \text{ mm}^{-3}$. It has been estimated that there are about 4×10^3 synaptic contacts per neuron [32]. Since about 50–100 such contacts belong to a single axon, the number of neighbors per neuron is about 40–100. Nevertheless, the essential physical property of the neocortex is that it is effectively two-dimensional. Thus the critical exponents characterizing the neural phase transition are the $d = 2$ exponents of directed percolation. These have been calculated in [1, 2], and [5], and appear in the linear response of the neocortical model to an impulsive stimulus, known to mathematicians as the *Green's function* and to physicists as the *propagator*. This takes the general form

$$G(x, t) \sim \lim_{\mu \rightarrow 0} \frac{x^2, t \rightarrow \infty}{|\mu|^{(\frac{1}{2} dz - \eta)}} \Phi(|\mu|^\nu t, |\mu|^{\nu z} x^2) \quad (44)$$

where $x = x_2 - x_1, t = t_2 - t_1, \mu = \mu_E$, and ν, η , and z are critical exponents that depend only on the dimension d . Φ is a universal scaling function which takes on different forms depending on whether μ is greater than or less than the critical value $\mu = 0$. Thus, in the subcritical case $\mu > 0$

$$G(x, t) \sim g^2 t^{-d/2} \exp(-x^2/4\alpha' t - \Delta t) \quad (45)$$

where $\Delta \sim |\mu|^\nu, \alpha' \sim |\mu|^{-\nu(z-1)}$, and $g^2 \sim |\mu|^{\nu[(1/2)d(z-1) - \eta]}$. In addition, the *susceptibility* is defined as

$$\chi = \iint d^d x dt G(x, t) \sim |\mu|^\gamma \quad (46)$$

where $\gamma = \nu(1 + \eta)$.

In the supercritical case $\mu < 0$

$$G(x, t) \sim M^2 \theta(vt - |x|) \quad (47)$$

where $v \sim |\mu|^{\nu(1-(1/2)z)}$, $M \sim |\mu|^\beta$, and $\beta \sim 1/2\nu((1/2)dz - \eta)$. $\theta(x)$ is the Heaviside step function.

In the critical case $\mu = 0$ equation (44) reduces to

$$G(x, t) \sim t^{-((1/2)dz - \eta)} [\Phi_c(x^2/t^2) + O(t^{-\lambda})] \quad (48)$$

where λ is another critical exponent describing the approach to scaling, and Φ_c can be calculated. (For more details see [3, 12, 27, 20].)

4.2.2. Renormalizing the driven neural action. We now assume that $n_H(\mathbf{x}, t) \neq 0$, so that the function s_E now takes the form

$$s(n_E, n_H) = k \left(Ln_E + b_H \frac{n_H}{\rho_S} \right). \quad (49)$$

The extra term in the current $s(n_E, n_H)$ adds extra terms to the neural action. However, we show in appendix that all but one of the additional terms do not survive the renormalization group process, so that the renormalized action for this case takes the form

$$S(s_E, s_H) = \iint d^d x dt [\tilde{s}_E (\partial_t + \mu_E - D_E \nabla^2) s_E + u_E \tilde{s}_E (s_E - \tilde{s}_E) s_E + v_E \tilde{s}_E s_H m_H] \quad (50)$$

where m_H is a scaled version of n_H .

We see that the additional term acts as a source to drive the dynamics away from the absorbing state $n_E = 0$. However, we assume that n_H is small, so that the lowest value reached by $n_E \approx 0$, i.e., the character of the neural activity remains close to DP.

4.2.3. Renormalizing the synaptic plasticity action. In similar fashion the action for neural plasticity given in equation (39) can be renormalized. The result derived in appendix is

$$S(s_H) = \iint d^d x dt [\tilde{s}_H \partial_t s_H + u_H \tilde{s}_H s_H m_H + v_H \tilde{s}_H (s_E - s_{E,0}) m_H]. \quad (51)$$

The result indicates that the renormalized synaptic weight fluctuation s_H is driven by m_H and depresses or potentiates, depending on the sign of the renormalized neural activity term $s_E - s_{E,0}$. By itself this behavior suggests that the fixed points of s_H oscillate between an upper and a lower state.

4.2.4. Renormalizing the combined action. Renormalization of the combined action is now simple. We simply add together the renormalized actions for the driven neural action and the synaptic plasticity. The result is

$$S(s_E, s_H) = \iint d^d x dt [\tilde{s}_E (\partial_t + \mu_E - D_E \nabla^2) s_E + u_E \tilde{s}_E (s_E - \tilde{s}_E) s_E + v_E \tilde{s}_E s_H m_H + u_H \tilde{s}_H \partial_t s_H + u_H \tilde{s}_H s_H m_H + v_H \tilde{s}_H (s_E - s_{E,0}) m_H]. \quad (52)$$

We note that the last term acts as a source or sink term for s_H , depending on the sign of $s_E - s_{E,0}$. It is not clear how this term affects the nature of the fluctuations in s_E .

5. Simulating the effects of fluctuations

In order to gain some insight into the behavior of the network dynamics beyond the mean-field regime we simulated the full system of coupled stochastic equations for a two-dimensional network comprising 60×60 excitatory neurons with nearest neighbor

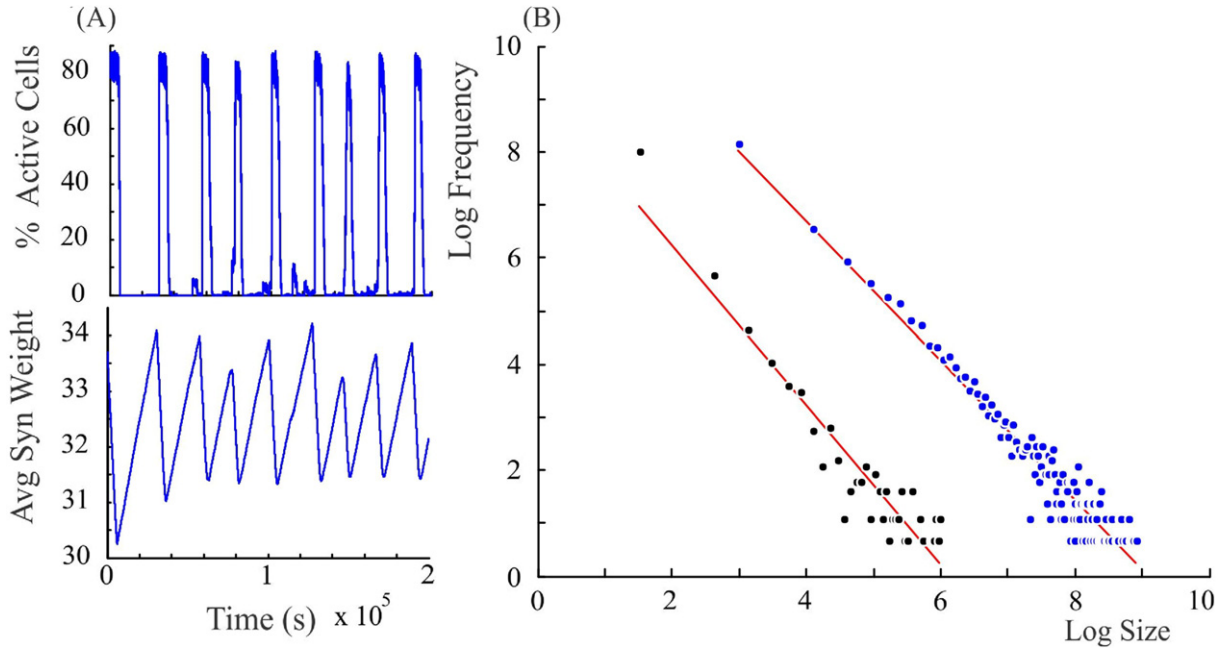


Figure 4. Neural state transitions between a ground state and an excited state in a two-dimensional network of 60×60 excitatory neurons with nearest neighbor connections. (A) Population activity and mean synaptic weight versus time. Activity levels display cyclic behavior with ‘UP’ and ‘DOWN’ states. (B) Avalanche distribution of DOWN states (black dots) and UP states (blue dots). Parameter values: $\kappa_{E,S} = 0.001$, $n_{E,0} = 0.2$, $w_E = 4$, $\alpha = 0.2$, $\beta = 0.002$, $g_E = 1$, and $I_{RH} = 1$. $f(x)$ is the function introduced in figure 2.

connections and toroidal boundary conditions, with each neuron receiving current pulses from all four neighbors, and also from an external cell through a modifiable synapse with weight function $w_H(\mathbf{x}, \mathbf{x}') = b_H \delta^d(\mathbf{x} - \mathbf{x}')$ such that $\int d^d \mathbf{x}' w_H \propto b_H$.

The simulations were run using the Gillespie algorithm for Markov processes (see [8]). The results are shown in figure 4. It will be seen that the population behavior shown in panel (A) replicates qualitatively that shown in the phase-plane of figure 3, and that the mean synaptic weight shows the oscillation-like character of the activity. Panel (B) shows the burst or avalanche-size distributions of the underlying spiking activity. Note that the fluctuations in spiking activity about the lower nullcline, or DOWN state, show a power-law distribution with a slope of about -1.51 , whereas those about the higher nullcline or UP state also show a power-law distribution with a slope of about -1.31 . This property is not seen in studies of the behavior of stochastic Wilson–Cowan equations for coupled $E-I$ networks with fixed synapses, reported in [8], in which the DOWN state shows power-law statistics, and the UP state shows Poisson statistics. This is just the opposite of the results reported in [26] and [25], in which UP states show power-law behavior, and DOWN states show Poisson behavior. (We will return to this point in section section 6.)

However, we note that the results of this simulation differ in certain respects from those obtained by Gil and Sornette [17]. In their paper they introduced simulations performed with a choice of time constants corresponding to the ratios $\alpha/\beta = 0.01$ and 100. Both simulations produced similar power laws for small avalanche sizes, but the

latter also produced an isolated large system-size avalanche, 1.25 orders of magnitude greater than the smaller avalanches. In the simulation considered here the ratio used is $\alpha/\beta g_E = 0.2/0.002 \times 1 = 100$. The result we find is that there are two branches of power-law distributed avalanches, corresponding to the UP and DOWN mean-field states. The UP avalanches are approximately three orders of magnitude greater than the DOWN ones.

6. Discussion

We have demonstrated that critical behavior in the form of power-law avalanche distributions can be obtained in a network of coupled excitatory stochastic Wilson–Cowan equations with a modifiable excitatory synapse in the input pathway. Such a system exhibits SOC. We have also shown that the slope of the power-law found in the UP states of the dynamics is consistent with that found in two-dimensional directed percolation ($\tau = 1.268$), within the experimental errors generated by the rather small size of our network simulation. Our results differ from those in [25] as well as those in [26]. However, these models differ in many respects from the model presented in this paper. Thus, Levina *et al* formulated a synaptic dynamics quite different from ours, but, interestingly, found that critical behavior required strong enough synapses, otherwise subcritical behavior occurred. In our simulations in which there was an excitatory anti-Hebbian synapse, we found that critical behavior occurred over a wide range of synaptic strengths. This property also differs from the results reported by Millman *et al* in which criticality also occurs over a wide range of synaptic strengths, but only for higher firing rates. These results might be related to the result reported above in which we found much larger avalanches in UP states than those found in DOWN states.

On the other hand, our results are not consistent with those we obtained earlier in Benayoun *et al* with a network of coupled excitatory and inhibitory cells with fixed synaptic weights. The key property in that study is that the balance between excitatory and inhibitory currents, equivalent to the net difference between the excitatory and inhibitory weights $w_E - w_I$ (equivalent to w_0 in the current formulation), is small, so that the net excitation of each cell is low, leading to critical DOWN but not UP states. This property did not seem to depend upon the overall connectivity of the network.

One other observation we can make concerns an application of the Ginzburg criterion [18]. One can derive this for stochastic Wilson–Cowan equations [41] in the form of the inequality

$$\left(\frac{w_2}{w_0}\right)^2 \gg \zeta \frac{|f^{(2)}| w_0 A}{f^{(1)}} L_D^{4-d}, \quad \text{where } L_D = \sqrt{\frac{f^{(1)} w_2}{2(\alpha - f^{(1)} w_0)}}$$

where ζ and A are constants, and L_D is the effective ‘diffusion’ length of the process. What is interesting about this formulation is that only the bulk parameters of the network, α , $f^{(1)}$, $|f^{(2)}|$, w_0 and w_2 , are required to reach a conclusion. If this inequality is violated then critical behavior occurs, otherwise mean-field behavior occurs. Thus, if $d < 4$, and if $f^{(1)} w_0 \rightarrow \alpha$, then critical behavior is likely. This shows that for a fixed value of α , the value of $f^{(1)} w_0$ controls the process. If w_0 , the total synaptic weight from neighboring neurons is small, then $f^{(1)}$ must be large. However, examination of figure 2 indicates that neural activity must then be low, so that criticality is to be expected in the DOWN state. Conversely, if w_0 is large then $f^{(1)}$ must be small. Again figure 2 indicates that the

resulting neural activity must then be high, so that criticality is now expected in the UP state. We conclude that the weight w_0 might be the key to whether or not UP and DOWN states are critical. It remains to incorporate the effects (if any) of the external stimulus n_H acting through the modifiable weight w_H into the Ginzburg criterion.

There are some experimental data to support the hypothesis that spontaneous or weakly stimulated brain activity exhibits near-critical behavior, and that strong external stimuli drive the activity into the mean-field regime. In fact there are a great many data supporting the hypothesis that the mean-field propagator correctly describes the essential features of large-scale strongly driven neocortical activity on many spatio-temporal scales. (See [15, 24, 28].) In addition, data on the statistical structure of large-scale spontaneous activity recorded in cortical slices by Beggs and Plenz [7], in particular the avalanche-size distribution of spontaneous activity in cortical slices, appear to fit the hypothesis of mean-field critical branching, which is consistent with the DP exponent of 1.5, for $d = 4$. But if the neocortex is two-dimensional our analysis suggests a smaller exponent. However, the neocortex is finite, so it is plausible that boundary effects change the exponent of the avalanche-size distribution near the surface from the smaller bulk exponent to one closer to 1.5 [21].

There are also many other differences in the formulation. In our study we do not have sparse randomly connected connectivity, or noisy input currents. It remains to be seen whether incorporation of these properties will make a difference in our results. We do know that such effects can trigger spontaneous symmetry breaking and collective effects in neural networks. (See, for example, [13, 22, 38], and [11].)

If these conclusions are correct, it is indicated that the approach we have outlined in this paper may prove to be of some value in the analysis of stochastic effects in neural networks.

Acknowledgments

The work reported in this paper was initially developed in large part with a former student Michael A Buice, now at the Allen Institute. We acknowledge helpful discussions with several of our colleagues at the University of Chicago, including Professors David Mazziotti and Greg Engel in the Department of Chemistry. We also thank Professor Nicholas Brunel in the Statistics Department for his help in the production and submission of this paper. Last but not least, we thank the referees for their constructive criticism of the first two submissions of this paper. The current work was supported (in part) by a grant to Wim van Drongelen from the Drs Ralph and Marian Falk Medical Trust.

Appendix

A.1. Expanding the weighting function

We can approximate the convolution operator as the truncation of an expansion in the moments

$$\mu_k = \int d^d x x^k w(\mathbf{x}) \tag{A.1}$$

so

$$w \star = \int d^d x' w(\mathbf{x} - \mathbf{x}') \approx w_0 + \frac{1}{2!} w_2 \nabla^2 + \dots \equiv L \quad (\text{A.2})$$

where

$$w(\mathbf{x}) \rightarrow w(r) = \frac{b}{\sigma^d} e^{-r/\sigma}, \quad \sigma = r_0 \quad (\text{A.3})$$

and

$$\begin{aligned} w_0 &= \int d^d x w(\mathbf{x}) = b \frac{d\Gamma(d)}{\Gamma(d/2 + 1)} \pi^{d/2}, \\ w_2 &= \int d^d x^2 w(\mathbf{x}) = b\sigma^2 \frac{d\Gamma(d+2)}{\Gamma(d/2 + 1)} \pi^{d/2}. \end{aligned} \quad (\text{A.4})$$

A.2. Renormalizing the neural action

We expand n_E about its mean value $\langle n_E \rangle = n_{E,cl}$, which satisfies equation (28) in the form

$$\partial_t n_{E,cl} = -\alpha n_{E,cl} + (\rho - n_{E,cl}) f[s(n_{E,cl})] \quad (\text{A.5})$$

where

$$s(n_{E,cl}) = k(w \star n_{E,cl} + b_H \star n_{H,cl}). \quad (\text{A.6})$$

Thus, $n_E \rightarrow n_E + n_{E,cl}$, $\tilde{n}_E \rightarrow \tilde{n}_E$, since $\tilde{n}_{E,cl} = 0$. Therefore, $s(n_E) \rightarrow s(n_E + n_{E,cl})$ and $f[s(n_E)] \rightarrow f[s(n_E + n_{E,cl})]$. It follows that $s(n_E + n_{E,cl}) = k(w \star (n_E + n_{E,cl}) + b_H \star (n_H + n_{H,cl})) = k(w \star n_{E,cl} + b_H \star n_{H,cl}) + k(w \star n_E + b_H \star n_H) = s(n_{E,cl}) + s(n_E)$, and therefore $f[s(n_E)] = f[s(n_{E,cl}) + s(n_E)]$. We next expand $f[s(n_E)]$ in a Taylor expansion about the mean-field value $n_{E,cl}$, noting that from equation (A.2) $s(n_E) = k(w \star n_E + b_H \star n_H) = k(Ln_E + b_H \star n_H)$.

In what immediately follows we assume that the external stimulus $n_H(\mathbf{x}, t) = 0$. It follows that

$$\begin{aligned} f[s(n_E)] &= f[kLn_{E,cl} + kLn_E] = f[kLn_{E,cl}] + f^{(1)}[kLn_{E,cl}]kLn_E \\ &\quad + \frac{1}{2} f^{(2)}[kLn_{E,cl}](kLn_E)^2 + \dots \end{aligned} \quad (\text{A.7})$$

However, because of normal ordering, equation (A.7) leads to the expression

$$f[s(n_E)] = \sum_m g_m (kLn_E)^m, \quad \text{where } g_m = \sum_{l=m} \frac{f^{(l)}}{l!} s_{l,m}. \quad (\text{A.8})$$

Since the leading terms of g_m are proportional to $f^{(m)}$, and given the assumed form for $f[s(n)]$ to be such that $f^{(1)} > 0$ and $f^{(2)} < 0$, then $g_m > 0$ for m odd, and $g_m < 0$ for m even.

In similar fashion we expand the function $n_E f[s(n_E)]$ as

$$n_E f[s(n_E)] = g[s(n_E)] = \sum_m h_m (kLn_E)^m, \quad \text{where } h_m = \sum_{l=m} \frac{g^{(l)}}{l!} s_{l,m}. \quad (\text{A.9})$$

However, we note that since $g^{(l)} = d^{(l)}g/ds^{(l)}$, $g^{(l)} = lf^{(l-1)} + f^{(l)}$, so that $h_m = g_m + g'_m$, where

$$g'_m = \sum_{l=m} \frac{f^{(l-1)}}{(l-1)!} s_{l,m} \quad (\text{A.10})$$

so we have

$$(\rho - n_E)f[s(n_E)] = (\rho - \bar{k}) \sum_m g_m (kLn_E)^m - \bar{k} \sum_m g'_m (kLn_E)^m = \bar{\rho}f[s(n_E)] - \bar{k}g[s(n_E)] \quad (\text{A.11})$$

where $\bar{k} = (kL)^{-1}$, $\bar{\rho} = \rho - \bar{k}$, and

$$g[s(n_E)] = \sum_m g'_m (kLn_E)^m. \quad (\text{A.12})$$

We also expand the functions $\exp(\pm \tilde{n}_E)$. The resulting action $S(n_E)$ takes the form

$$S(n_E) = \iint d^d x dt [\tilde{n}_E(\partial_t + \alpha - \bar{g}_1 kL)n_E - \frac{1}{2}\tilde{n}_E^2(\alpha + \bar{g}_1 kL)n_E + \tilde{n}_E|\bar{g}_2|(kL)^2 n_E^2 + \frac{1}{2}\tilde{n}_E^2|\bar{g}_2|(kL)^2 n_E^2 + \dots] \quad (\text{A.13})$$

where $\bar{g}_m = \bar{\rho}g_m - \bar{k}g'_m$.

It follows that for functions $n_E(\mathbf{x}, t)$ that vary slowly in space $\frac{1}{2}w_2\nabla^2 n_E$ is small compared to $w_0 n_E$, so that in most expressions the terms proportional to $\nabla^{2m} n_E^m$ can be neglected. However, this is not always the case for $m = 1$. Thus, the first term can be written approximately as $\tilde{n}_E(\partial_t + \alpha - \bar{g}_1 k w_0 + \frac{1}{2}\bar{g}_1 k w_2 \nabla^2)n_E = \tilde{n}_E(\partial_t + \mu_E - D_E \nabla^2)n_E$, where $\mu_E = \alpha - \bar{g}_1 k w_0$ and $D_E = \frac{1}{2}\bar{g}_1 k w_2$.

Therefore, the expression for the action is now reduced to the form

$$S(n_E) = \iint d^d x dt [\tilde{n}_E(\partial_t + \mu_E - D_E \nabla^2)n_E - \tilde{n}_E^2 G_1 n_E + \tilde{n}_E G_2 n_E^2 + \frac{1}{2}\tilde{n}_E^2 G_2 n_E^2 + \dots] \quad (\text{A.14})$$

where $G_1 = 1/2(\alpha + \bar{g}_1 k w_0)$, $G_2 = |\bar{g}_2|k^2 w_0^2$. We need to demonstrate that the last term in $S(n_E)$, i.e., $\frac{1}{2}\tilde{n}_E^2 G_2 n_E^2$, and all higher-order terms, are *irrelevant* in the sense of the renormalization group.

The renormalization group (RG) analysis is carried out via dimensional analysis. It can be shown that all the terms in $S(n_E)$ are zero-dimensional when integrated over d -dimensional space and over time, i.e., $[d^d x dt] = L^{-(d+2)}$ and (any term in the integrand) = L^{d+2} . However, as it stands, $[n_E] = L^d$, but $[\tilde{n}_E] = L^0$, so that $[\tilde{n}_E n_E] = L^{0+d} = L^d$. This is not suitable for the scaling analysis implemented in the RG process. We therefore introduce a new *scaling*,

$$\tilde{s}_E = \sqrt{\frac{G_1}{G_2}} \tilde{n}_E, \quad s_E = \sqrt{\frac{G_2}{G_1}} n_E \quad (\text{A.15})$$

such that $\tilde{s}_E s_E = \tilde{n}_E n_E$, where $[G_2/G_1] = L^{-d}$. The effect of this scaling is that both \tilde{s}_E and s_E have dimension $L^{d/2}$. Let

$$\sqrt{G_1 G_2} = u_E. \quad (\text{A.16})$$

The net effect of this scaling transformation is that

$$S(s_E) = \iint d^d x dt [\tilde{s}_E(\partial_t + \mu_E - D_E \nabla^2)s_E + u_E \tilde{s}_E(s_E - \tilde{s}_E)s_E + \dots]. \quad (\text{A.17})$$

The constants of all higher-order terms have dimensions such that the dimension of their ratio to the coupling constant u scales as $L^{-\beta d}$, where $\beta > 0$, so they become *irrelevant* as $L \rightarrow \infty$. It follows that

$$S(s_E) = \iint d^d x dt [\tilde{s}_E(\partial_t + \mu_E - D_E \nabla^2)s + u_E \tilde{s}_E(s_E - \tilde{s}_E)s_E] \quad (\text{A.18})$$

is the *renormalized action* of the large-scale neural activity of a single neural population.

A.3. Renormalizing the synaptic plasticity action

We now proceed to renormalize the action $S(b_H)$ just as we renormalized $S(n_E)$. We therefore expand the exponential term in equation (40) and rewrite $S(b_H)$ in the form

$$S(b_H) = \iint d^d x dt \left[\tilde{b}_H \partial_t b_H + H_1 \tilde{b}_H b_H n_H - \frac{1}{2} H_1 \tilde{b}_H^2 b_H n_H + H_2 (n_E - n_{E,0}) \tilde{b}_H \frac{n_H}{\rho_S} + H_2 (n_E - n_{E,0}) \tilde{b}_H^2 \frac{n_H}{\rho_S} \right] \quad (\text{A.19})$$

where $H_1 = \beta g_E |\kappa_{E,S}| / \rho_S$ and $H_2 = \beta g_E$.

We now introduce the scaling

$$\tilde{s}_H = \sqrt{\frac{H_2}{H_1}} \tilde{b}_H, \quad s_H = \sqrt{\frac{H_1}{H_2}} b_H \quad (\text{A.20})$$

such that $\tilde{s}_H s_H = \tilde{b}_H b_H$ and $[H_1/H_2] = L^{-d}$. This scaling is analogous to the scaling of n and \tilde{n} which we carried out earlier for neural activities. As before, the effect of this scaling is that both \tilde{s}_H and s_H have dimension $L^{d/2}$.

Let

$$\sqrt{H_1 H_2} = u_H, \quad H_1 = 2\tau_H \quad (\text{A.21})$$

and recall that equation (A.15) scales n_E to $\sqrt{G_1/G_2} s_E$.

Following the procedure outlined earlier we can calculate which terms in the transformed action $S(s_H)$ become irrelevant under scaling transformations. The resulting renormalized synaptic plasticity action takes the form

$$S(s_H) = \iint d^d x dt [\tilde{s}_H \partial_t s_H + u_H \tilde{s}_H s_H m_H + v_H (s_E - s_{E,0}) \tilde{s}_H m_H] \quad (\text{A.22})$$

where

$$v_H = \sqrt{\frac{G_1}{G_2}} \frac{H_2}{\rho_S} \quad \text{and} \quad m_H = \sqrt{\frac{H_1}{H_2}} n_H \quad (\text{A.23})$$

so that v_H has the same scaling dimension as u_H .

A.4. Renormalizing the driven neural action

We now assume that $n_H(\mathbf{x}, t) \neq 0$, so that the function s_E now takes the form

$$s(n_E, n_H) = k \left(Ln_E + b_H \frac{n_H}{\rho_S} \right). \quad (\text{A.24})$$

It follows that the function $(\rho - n)f[s(n_E, n_H)]$ can now be expanded in the normal ordered form

$$(\rho - n)f[s(n_E, n_H)] = \sum_m \bar{g}_m \left((kLn_E)^m + \left(kb_H \frac{n_H}{\rho_S} \right)^m \right) + \bar{h}_2 kLn_E b_H \frac{n_H}{\rho_S} + \dots \quad (\text{A.25})$$

where $\bar{h}_2 = \bar{\rho}f^{(2)}$. The effect of this is to generate additional terms in the neural action. We therefore expand equation (A.25) and retain only the first few terms because all the terms which give rise to 4-vertices or higher will not survive the renormalization group procedure (see [33]). The extra terms we include in the action are

$$\left(\tilde{n}_E + \frac{1}{2} \tilde{n}_E^2 \right) \left(\bar{g}_1 \left(kb_H \frac{n_H}{\rho_S} \right) - |\bar{g}_2| \left(kb_H \frac{n_H}{\rho_S} \right)^2 - |\bar{h}_2| \left(kLn_E kb_H \frac{n_H}{\rho_S} \right) \right). \quad (\text{A.26})$$

However, only the term $\tilde{n}_E \bar{g}_1 kb_H n_H / \rho_S$ survives the RG process as $v_E \tilde{s}_E s_H m_H$, where v_E is a constant with the same scaling dimension as v_H and u_H .

A.5. Renormalizing the combined action

Renormalization of the combined action is now simple. We simply add together the renormalized actions for the driven neural action and the synaptic plasticity. The result is

$$S(s_E, s_H) = \iint d^d x dt [\tilde{s}_E (\partial_t + \mu_E - D_E \nabla^2) s_E + u_E \tilde{s}_E (s_E - \tilde{s}_E) s_E + v_E \tilde{s}_E s_H m_H + \tilde{s}_H \partial_t s_H + u_H \tilde{s}_H s_H m_H + v_H (s_E - s_{E,0}) \tilde{s}_H m_H] \quad (\text{A.27})$$

where u_E, v_E and u_H, v_H are renormalized constants, all with the scaling dimension $L^{2-d/2}$.

References

- [1] Abarbanel H and Broznan J, 1974 *Phys. Lett. B* **48** 345
- [2] Abarbanel H, Broznan J, Schwimmer A and Sugar R, 1976 *Phys. Rev. D* **14** 632
- [3] Abarbanel H, Broznan J, Sugar R and White A, 1975 *Phys. Rep.* **21** 119
- [4] Alstrom P, 1988 *Phys. Rev. A* **38** 4905
- [5] Amati D, Marchesini G, Ciafoloni M and Parisi G, 1976 *Nucl. Phys. B* **114** 483
- [6] Bak P, Tang C and Wiesenfeld K, 1988 *Phys. Rev. A* **38** 364
- [7] Beggs J and Plenz D, 2003 *J. Neurosci.* **23** 11167
- [8] Benayoun M, Cowan J, van Drongelen W and Wallace E, 2010 *PLoS Comput. Biol.* **6** e1000846
- [9] Buice M A and Cowan J D, 2007 *Phys. Rev. E* **75** 051919
- [10] Buice M and Cowan J, 2009 *Prog. Biophys. Theor. Biol.* **99** 53
- [11] Butler T, Benayoun M, Wallace E, van Drongelen W, Goldenfeld N and Cowan J, 2012 *Proc. Nat. Acad. Sci.* **109** 606
- [12] Cardy J and Sugar R, 1980 *J. Phys. A: Math. Gen.* **13** L423
- [13] Chu P H, Milton J and Cowan J D, 1994 *Int. J. Bifurcation. Chaos* **4** 237
- [14] Cowan J D, 1991 *Advances in Neural Information Processing Systems* Vol 3, ed D Touretzsky, R Lippman and J Moody (San Mateo, CA: Morgan Kaufmann) pp 62–8

- [15] Delisle Burns B, 1951 *J. Physiol.* **112** 156
- [16] Doi M, 1976 *J. Phys. A: Math Gen.* **9** 1465
- [17] Gil L and Sornette D, 1996 *Phys. Rev. Lett.* **76** 3991
- [18] Ginzburg V, 1960 *Sov. Phys.—Solid State* **2** 1824
- [19] Glauber R, 1963 *Phys. Rev. Lett.* **10** 84
- [20] Hinrichsen H, 2000 *Adv. Phys.* **49** 815
- [21] Janssen H K and Täuber U C, 2005 *Ann. Phys.* **315** 147
- [22] Jung P and Mayer-Kress G, 1995 *Chaos* **5** 458
- [23] Kilman V, van Rossum M and Turrigiano G, 2002 *J. Neurosci.* **22** 1328
- [24] Lampl I, Reichova I and Ferster D, 1999 *Neuron* **22** 361
- [25] Levina A, Herrmann J and Geisel T, 2007 *Nature Phys.* **3** 857
- [26] Millman D, Mihalas S, Kirkwood A and Niebur E, 2010 *Nature Phys.* **6** 801
- [27] Munoz M, Dickman R, Vespignani A and Zapperi S, 1999 *Phys. Rev. E* **59** 6175
- [28] Nauhaus I, Busse L, Carandini M and Ringach D, 2009 *Nature Neurosci.* **12** 70
- [29] Ohkubo J, 2010 *J. Stat. Phys.* **139** 454
- [30] Peliti L, 1985 *J. Physique* **46** 1469
- [31] Schrödinger E, 1926 *Naturwissenschaften* **14** 664
- [32] Stevens C, 1989 *Neural Comput.* **1** 473
- [33] Täuber U C, Howard M and Vollmayer-Lee B P, 2005 *J. Phys. A: Math. Gen.* **38** R79
- [34] Van Kampen N, 1981 *Stochastic Processes in Physics and Chemistry* (Amsterdam: North-Holland)
- [35] van Wijland F, 2001 *Phys. Rev. E* **63** 022101
- [36] Vogels T, Sprekeler H, Zenke F, Clopath C and Gerstner W, 2011 *Science* **334** 664
- [37] Han V Z, Grant K and Bell C, 2000 *Neuron* **24** 611
- [38] Wang J, Kádár S, Jung P and Showalter K, 1999 *Phys. Rev. Lett.* **82** 855
- [39] Wilson H and Cowan J, 1972 *Biophys. J.* **12** 1
- [40] Wilson H R and Cowan J D, 1973 *Kybernetik* **13** 55
- [41] Buice M and Cowan J D, 2007 unpublished